Part C

SURFACE PROCESSES

CHAPTER 6

Deposition and Dissolution Processes

6.1 INTRODUCTION

Electrochemical processes taking place entirely in the solution phase (both *Ox* and *R* are soluble in the electrolyte medium—Chapters 3 to 5) of course belong to a very important and interesting class. However, there are equally important processeses that take place predominantly at the electrode or the solid phase. For convenience, a solid phase process may loosely be defined as one in which "a new solid phase is formed on the surface, a solid phase dissolves into the electrolyte or a change in the redox state of the solid phase occurs due to charge transfer." Cathodic deposition of metals, anodic formation of metal oxides, sulphides or any insoluble metallic salts and cathodic or anodic formation of polymer films are examples of formation of new phases due to charge transfer (Chapters 6 to 8). Most of these new phases formed can be dissolved by sweeping the potential in the opposite direction. For example, a deposited metal may be dissolved by anodic oxidation. Conversion of lead sulphate to lead dioxide and reduction of lead dioxide to lead sulphate in the solid state is a well-known example of surface redox reaction (Chapter 10). Throughout this part (Chapters 6 to 10) such solid phase processes are discussed in some detail.

For dealing with solid phase processes more phenomenological models are needed when compared with the ones used in describing solution phase processes. Interaction between the metal electrode surface and the new phase being formed must be considered (Section 6.3.4). The new phase may grow at random or by nucleation process (Chapters 7 and 8). In the growth of anodic phases on solids, the solid state growth mechanisms must be considered (Chapter 8). Solid phase redox processes also pose some challenging problems at the model level itself (Chapters 9 and 10).

However, one can still describe a number of such solid phase electrochemical processes with the three phenomenological components introduced in the discussion of solution phase processes, that is, charge transfer, chemical reactions and mass transport. Some modifications of course must be considered in the physical description of the processes. For example, there are slight modifications in the Nernst equation of charge transfer (Section 6.2.1). The chemical reactions in the electrolyte (Section 6.2.2) are of course similar. The same molecular model may be used to describe the chemical interactions between metals (Section 6.2.3). In the concept

of mass transport, the limited or finite diffusion layer shall be encountered for the first time (Section 6.2.4). With these models, a number of electrochemical processes can be studied by LSV, CV and especially by stripping voltammetry (Section 6.3). Some case studies (Section 6.4) and analytical applications (Section 6.5) also are discussed.

In a sense therefore one may consider this chapter on solid phase processes as a link between the solution phase processes discussed earlier (Chapters 3 to 5) and the solid phase processes to be considered later (Chapters 7 to 10) where new model components are introduced. Proper understanding at this level of solid phase processes is a prerequisite to the more sophisticated models considered later.

Historically, interestingly the first CV experiment was the study of a metal deposition-dissolution process on Hg electrode [1]. But this study employed a *DME* which is not easily amenable to theoretical treatments for LSV and CV experiments. Hg plated solid electrodes [2, 3] were used as stationary Hg electrodes for quite sometime. The hanging mercury drop electrode (HMDE) was thoroughly characterized later (4, 5). Solid metal [6] and carbon [7] electrodes were also used for such studies. Many new developments have taken place in the experimental methods as are discussed later.

From the theoretical angle the Randles [8] and Seveik [9] derivation of LSV behaviour perfectly holds for metal deposition processes on relatively thick mercury electrodes (Section 6.3.1). The deposition process on a solid electrode was treated in 1953 [10]. The theoretical treatment for limited diffusion layer was first considered more than a decade later [11]. A number of newer developments are taking place even today in the theoretical treatments for new process models as well as for new experimental methods (Section 6.3).

6.2 THE MODEL

6.2.1 THE CHARGE TRANSFER

First consider the most widely studied solid phase process, the deposition and dissolution of metals. If M^{n+} denotes the metal ion and M the metal, then

$$M^{n+} + ne \rightleftharpoons M \tag{6.1}$$

This reaction is of course very similar to Ox/R reactions in solution discussed hitherto (Chapters 3 to 5). However, there is an important difference. The reduced metal M is not soluble in the electrolyte. It preferably interacts with the electrode material. Three distinct possibilities must now be considered depending on the electrode material selected.

a) If the electrode material exists in the form of a liquid metal (say Hg) and the reduced species M is freely soluble in it, one has the first interesting situation. If the charge transfer is reversible, one can write an equation very similar to the Nernst equation of Ox/R couple (equation 3.27).

$$E = E^f + \frac{RT}{nF} \ln \frac{C_{M^{n+}}(o, t)}{C_M(o, t)} \qquad 6.2$$

In this boundary condition expression for reversible charge transfer, there are the surface concentration expressions for $C_{M^{n+}}(o, t)$ and $C_M(o, t)$. The surface concentration of metal ion is related to its bulk concentration in the electrolyte. On the other hand, the surface concentration of metal M is now related to the bulk concentration of the same metal in the liquid electrode (Hg).

The rate expression for irreversible charge transfer is also very similar to that of the Ox/R couple in solution,(equations 4.45, 4.46)

$$i = nF\,A\,k_h^o\,C_M n^+(o,t) \exp\{-\alpha n_a f(E - E^f)\} \qquad 6.3$$

for totally irreversible charge transfer and

$$i = nF\,A\,k_h^o \left[C_M n^+(o,t) \exp\left\{-\alpha n_a f(E - E^f)\right\} - C_M(o,t) \exp\left\{(1-\alpha)\, n_a f(E - E^f)\right\}\right] \qquad 6.4.$$

for quasireversible charge transfer. Except for the fact that $C_M(o, t)$ now must be correlated with the bulk concentration of the liquid electrode, all the parameters and their significance are similar to the Ox/R reactions discussed earlier (Section 4.2).

b) M cannot move into the the electrode bulk if the base electrode is a solid. If in this case the depositing metal is the same as the substrate (say Ag^+ ion on Ag electrode) there is another simp-

lification. Equations 6.2, 6.3 and 6.4 of course hold for a reversible, irreversible and quasi-reversible charge transfer respectively. But now the concentration of M on the surface of the metal can be taken as unity, that is,

$$C_M\,(o, t) = 1 \qquad 6.5$$

This type of boundary condition is never encountered in solution phase processes but has very important effects in the LSV and CV behaviour of metal deposition-dissolution processes (Section 6.3.3).

It is worthwhile to understand the correct meaning of equation 5. The surface concentration at the electrode surface remains constant even though the metal deposition takes place continuously. This is so because at every instant of deposition the maximum concentration of M at the surface is constant and that is equal to a monolayer. In a stricter sense of course it is the activity of the electrode that remains constant.

When equations 6.3 and 6.4 are used for deposition/dissolution processes on a solid electrode, one also assumes that the surface area of the electrode remains constant throughout. (The electrode area A is independent of time). This is possible only if the deposition is perfectly uniform on a perfectly defined substrate electrode material. This is highly unlikely on solid electrode. However, models of surface processes that incorporate change of electrode area with time would be considered later (Chapter 8).

c) If the metal M is deposited onto a different solid metal electrode or even a non-metallic electrode such as carbon, there is another situation. $C_M\,(o, t)$ cannot be taken as 1 until the electrode material is covered by at least one monoatomic layer of M. Thus during deposition process, for example, one notices that $C_M\,(o, t)$ increases from 0 to 1 and then remains constant at one. During the anodic dissolution the $C_M\,(o, t)$ would remain at one till the bulk of the electrode material excepting a monolayer of M is dissolved. Then $C_M\,(o, t)$ would drop from one to zero.

Now from euqation 6.2 if $C_M\,(o, t)$ is less than one, E or the deposition potential can be much more positive when compared with E^o even if $C_M n^+\,(o, t)$ is maintained at unity. Hence in LSV and CV a separate monolayer formation-dissolution peak may be noticed before the bulk deposition-dissolution peak [1, 2]. We shall

only consider very briefly this monolayer process here with reference to its link with the bulk deposition process (Section 6.2.4). A more thorough and detailed discussion of monolayer formation/dissolution processes are reserved for the next chapter.

In this section so far the deposition and dissolution of metals are considered (equation 6.1). Of course this is the most widely considered solid phase formation process. However, solid phases may be formed by oxidation processes. Metals can, for example, form metallic oxides or sulphides. Insoluble salts such as mercurous halides may be formed by anodic oxidation in the appropriate halide media. These processes may in general be written as

$$M - X + ne \rightleftharpoons M + nX^{-} \qquad 6.6$$

In this equation X^{-} refers to the anion in solution. For example, if X^{-} is OH^{-}, O^{2-}, S^{2-}, Cl^{-} and I^{-}, one may observe the formation of metallic hydroxide, oxide, sulphide, chloride and iodide respectively. (Since the film is formed by an anodic process, many used to write this reaction in the reverse direction. However, IUPAC convention requires the writing of any half cell reaction as a reduction process and refer the standard reduction potential E^{o} to the reaction using equations similar to 6.2).

The charge transfer equilibrium and rate expressions of the anodic processes are very similar to those discussed above (equations 6.2 to 6.4). For these cases the $C_{M^{n+}}(o, t)$ and $C_M(o, t)$ must be replaced by $C_M X^{-}(o, t)$ and $CX^{-}(o, t)$ respectively (Since these are the O_x and R species for reaction 6.6).

Although these anodic film formation and their cathodic stripping are recently employed very extensively in electroanalysis, most of the theoretical literature published earlier and even today primarily consider the metal deposition processes. And hence this chapter shall primarily deal with such processes. However, these expressions can readily be used for reaction 6.6 with due consideration to the concentration of the correct reactant and product.

6.2.2 CHEMICAL REACTIONS IN SOLUTION

In solution phase processes, both O_x and R species can interact with molecular or ionic species in solution. But in solid phase

process the oxidized species (M^{n+}) alone can interact with the species in the electrolyte solution. However, the reduced species (M) can chemically interact with the atoms of the electrode material. After considering the chemical interactions in solution here, the interactions shall be considered in the electrode material in the next section (Section 6.2.3).

Consider the complex formation of M^{n+} with p molecules of a ligand X.

$$(MX_p)^{n+} = M^{n+} + pX \qquad 6.7$$

Usually in metal deposition processes, the complex species would be more stable and hence much more difficult to reduce electrochemically. The equilibrium constant for this reaction may be written as

$$K = \frac{C_{M^{n+}} \cdot C_X^p}{C_{MX_p^{n+}}} \qquad 6.8$$

Note that this chemical equilibrium is very similar to the preceding chemical equilibrium case ($Z/Ox/R$) represented in Table 3.1 for a solution phase process. The $E_{1/2}$ for this process may be written from Table 3.1 noting that Z is MX_p^{n+} and Ox is M^{n+} and R is M in the present case.

$$E_{1/2} = E^o + \frac{0.059}{n} \log K + \frac{0.059}{n} \log \frac{C_{MX_p^{n+}}}{C_M \cdot C_X^p} \qquad 6.9$$

This equation shows that $E_{1/2}$ would shift cathodically by $(59.2/n)$ mV (at 298 K) if p the number of ligands involved in the metallic complex is 1 for each ten-fold increase of ligand concentration X. If $p = 2$, the shift would be $(118.4/n)$ mV, if $p = 3$ the shift would be $(177.6/n)$ mV and so on. Hence from $E_{1/2}$ versus log X slope one can evaluate p. If the $E_{1/2}$ of uncomplexed species is known, the instability constant of the complex formation (K) may be evaluated.

The ligand number p may itself vary with the concentration of ligand, say, from 1 at low concentration of X to 2, 3 or even 4 at higher concentrations.

$$MX_4^{n+} \underset{X}{\overset{K_4}{\rightleftharpoons}} MX_3^{n+} \underset{X}{\overset{K_3}{\rightleftharpoons}} MX_2^{n+} \underset{X}{\overset{K_2}{\rightleftharpoons}} MX^{n+} \underset{X}{\overset{K_1}{\rightleftharpoons}} MX^{n+} \qquad 6.10$$

By obtaining proper $E_{1/2}-\log X$ plots with varying slopes, one can obtain these stepwise equilibrium constants. Study of the equilibrium properties of metallic complexes is very extensively dealt with in polarographic literature [13–15]. All these treatments may be directly used as long as they employ $E_{1/2}-\log X$ relations, for LSV and CV methods as well. The $E_{1/2}$ of course must be obtained from E_p and / or $E_{p/2}$ measurements using appropriate relations (Section 6.3.1).

In the discussions in this section, one has so far assumed that the dissociation of metal complexes is an equilibrium process. Most of the polarographic studies are also confined to this type of studies. The rate of the forward reaction (that is, metal complex dissociation, equation 6.7) can also influence the overall charge transfer. The kinetics of such preceding chemical reactions can be studied using the models developed for *CE* reactions (Section 5.3.1). Transient techniques must be suitable for studying such apparently fast reactions. However, very little effort is noticed in this direction.

6.2.3 THE CHEMICAL INTERACTIONS OF METALS

If the substrate electrode is a solid, the depositing metal atoms (M) would interact only with the surface atoms of the substrate. Such interactions at the monolayer level are considered in the next chapter. In this section our discussions are confined to the interactions of deposited metal with the bulk of the liquid electrode and that too primarily with Hg electrode which has received considerable attention.

The interactions of depositing metals with another liquid metal electrode may be considered at three distinct levels at least from the physico-chemical point of view:

a) Some depositing metals may have very little chemical interaction with mercury. They would simply dissolve in the bulk of the liquid metal. The solubility of individual metals may of course vary (Section 6.4.3). For such metals the $E_{1/2}$ of reduction on Hg would be very close to the E^f of the same metal/metal ion couple (that is, the deposition potential of M^{n+} on the electrode M and on the Hg electrode would be the same). If the amount of M deposited exceeds its solubility in Hg the electrode loses its homo-

geneity. Separate solid phases of M would form in Hg and the voltammetric response would become less accurate.

b) Most of the active metals when deposited on Hg form stable chemical interactions with Hg. The metal-mercury interactions of this type may be considered as the chemical reaction following the charge transfer (6.1).

$$M + \text{Hg} \rightleftharpoons M - \text{Hg} \qquad 6.11$$

This process is generally termed as amalgam formation.

The reaction scheme consisting of equations 6.1 and 6.11 may be viewed as an *EC* process. The chemical step (equation 6.11) is considered as an equilibrium step, the product of charge transfer is stabilized by this step, and hence the $E_{1/2}$ is shifted in the positive direction compared with the standard reduction potential of M^{n+}/M reaction. The positive shift of the reduction potential can be as high as 1 volt. Note that these ideas are based on the generalization of influence of chemical reactions on charge transfer discussed earlier (Section 3.2.2).

c) Another interesting situation is encountered when more than one metal is deposited on to Hg. Suppose a metal M_2 is deposited on a Hg electrode containing M_1. Now M_2 can interact with Hg (amalgam formation) or M_2. The second process is termed as intermetallic compound formation. This sequence also can be considered as an *EC* process as follows:

$$M_2^{n+} + ne \rightleftharpoons M_2 \qquad 6.12$$

$$M_2 + M_1 \rightleftharpoons M_2 - M_1 \qquad 6.13$$

Now if the E^o values of M_1^{n+}/M couple and M_2^{n+}/M_2 couple are E_1^o and E_2^o respectively, the $E_{1/2}$ value of this intermetallic compound lie in-between the two. As is noted later (Section 6.4.3) extensive studies of the redox behaviour of amalgams and intermetallic compounds have been made. However, the scope for further work in the same line is quite extensive.

As in the case of electrolytes, the chemical interactions in the metallic electrode have also been treated so far generally in a thermodynamic angle. Interestingly the kinetics of the intermetallic compound formation reaction (equation 6.13) was measured using cyclic voltammetry during 1960 [16]. Unfortunately, however, these

studies were not pursued further. The methods described for the study of the kinetics of *EC* schemes (Section 5.3.2) can be used for the study of intermetallic compounds as well.

6.2.4 MASS TRANSPORT AND LIMITED DIFFUSION LAYER

During electrodeposition/dissolution processes also we encounter mass transport. First consider the simplest case of electrodeposition of metal (M) on a planar liquid electrode (Hg film on Ag or glassy carbon for example). The transport equation under purely diffusion controlled conditions are again the same as 3.28 and 3.29 for Ox/R species. But tne corresponding species here are M^{n+}/M. The Fick's second law may thus be written.

$$\frac{\partial C_{M^{n+}}(x, t)}{\partial t} = D \frac{\partial^2 C_{M^{n+}}(x, t)}{\partial x^2} \qquad 6.14$$

$$\frac{\partial C_M(x, t)}{\partial t} = D \frac{\partial^2 C_M(x, t)}{\partial x^2} \qquad 6.15$$

But the boundary conditions for solving these equations are quite different. This arises basically because the diffusion of M^{n+} and M actually takes place at two opposite directions from the interface

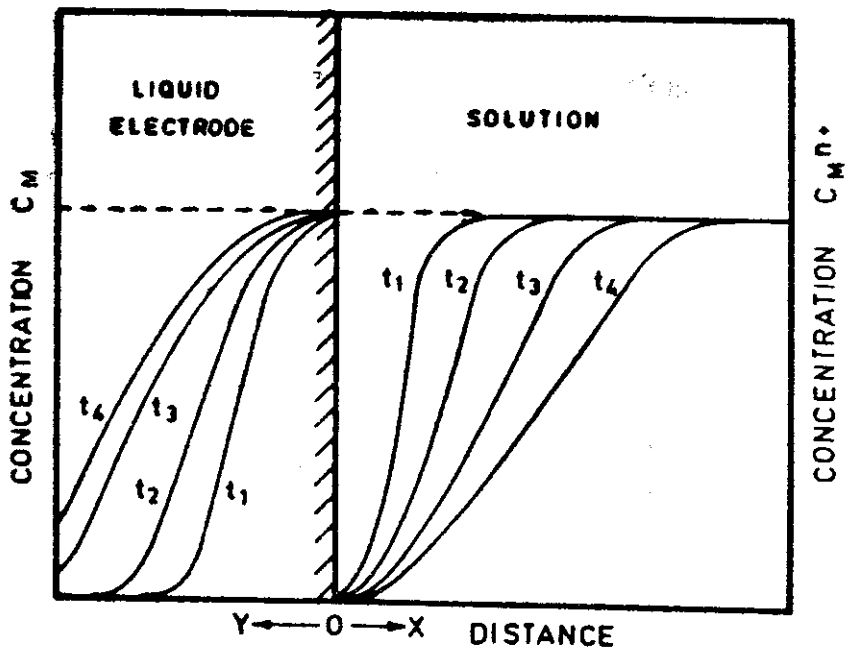

Fig. 6.1 Diffusion layers in the solution (x 0) and electrode side of the interface at various times, $t_1 < t_2 < t_3 < t_4$.

(Fig. 6.1). The concentration profiles of M^{n+} and M at various times when the deposition potential is kept at sufficiently cathodic where $C_M n^+ (o, t)$ would always be zero (peak current region of the voltammogram) are presented in Fig. 6.1. The concentration of M^{n+} changes from its bulk value ($x \to \alpha$) to zero at the interface ($x = 0$). The concentration of M at the interface ($y = 0$) is equal to the bulk concentration of M^{n+}. It slowly diffuses with the bulk of the liquid metal whose thickness is $l (y = l)$. With increasing time the diffusion layer thickness slowly increases for both M^{n+} and M.

Now two important consequences arise because of the presence of two diffusion layers on both sides of the interface even for a planar electrode.

a) The oxidized (M^{n+}) and reduced species here are moving in two different media of entirely different properties and so one can no longer assume that $D_{Mn+} = D_M$ as one did in solution phase processes. This is an important consideration for predicting the correct shapes of cyclic voltammograms. Experimental measurements have clearly indicated that the diffusion coefficients can be different.

b) Another and even more important difference is the fact that the thickness of the diffusion layers is entirely different. In the solution side, there is a diffusion layer which can be very large. This layer can be increased at will by increasing the inter-electrode distance. But it is neither possible nor advisable to have very thick films. The radius of most of the HMDE electrodes would be 1 mm. Mercury film electrodes (*MFE*) are purposefully made to be even thinner (for analytical reasons, see later). Hence the liquid electrode material offers only a limited or finite layer for the diffusion of metals.

Assume that the thickness of the electrode is 1 cm This is an invariant in a particular experimental situation. However, one can change the thickness of the diffusion layer $L (t)$ by varying the reaction time of experiment (Fig. 6.1). $L (t)$ can be easily evaluated using the expression

$$L (t) = (2 D t)^{1/2} \qquad 6.16$$

If it is assumed that the D_M in the liquid metal is 10^{-5} cm^2/sec and if the time of sweep is 5 sec (potential sweep rate of 100 mV/sec

through a potential range of 500 mV), $L(t)$ is found to be 10^{-2} cm. Now compared with the thickness of HMDE (10^{-1} cm) this is an order of magnitude smaller. Since the diffusion layer thickness in this case is very much smaller when compared with the thickness of the electrode, one can still assume that semi-infinite linear diffusion conditions prevail in the electrode meterial as well. This assumption is valid if very short time scales or very high sweep rates are employed.

The cases where semi-infinite linear diffusion prevails both in solution and in the liquid electrode are the easiest ones to treat for LSV and CV techniques. In fact the derivations of solution phase processes are directly applicable in this case (Section 6.3.1). Some noticeable differences of course exist when correction for spherical diffusion effects on HMDE are considered (Section 6.3.1b).

The diffusion layer thickness calculated above (10^{-2} cm) is closer to or even larger than the thickness of thin mercury film electrode (5×10^{-3} cm to 8×10^{-3} cm). The semi-infinite linear diffusion model is no longer valid in this case. For such cases one must introduce appropriate boundary conditions to equation 6.15 for proper solution. The voltammetric responses then depend on the thickness l of the electrode (Section 6.3.2).

The mass transfer expression is very much simplified when deposition/dissolution processes on solid electrodes are considered. $C_M(o, t)$ at the surface becomes unity and constant as discussed above (Section 6.2.1). The voltammetric response for such systems shall be considered in Section 6.3.3.

One specific aspect of deposition/dissolution process has attracted greater attention because of its analytical importance. This of course is the stripping voltammetry. In this method the metal ions are first reduced at a constant cathodic potential and a concentration of metal atoms in the electrode phase is achieved. A rest time is then usually allowed to ensure uniform concentration of metal in the electrode. This is followed by anodically stripping of the deposited metals. The voltammetric responses of such anodic stripping processes have been studied in greater detail. These aspects shall be considered in Section 6.3.4.

6.3 THE METHOD

From the above discussions it is quite evident that the voltammetric responses of deposition dissolution processes would depend very much on the nature of the substrate electrodes used. Hence the voltammetric responses shall be discussed under the three limiting conditions, that is, the thick liquid electrodes (Section 6.3.1), thin film liquid electrodes (Section 6.3.2) and solid electrodes (Section 6.3.3). Stripping analysis on these types of electrodes are then considered (Section 6.3.4).

6.3.1 VOLTAMMETRY AT SEMI-INFINITE DIFFUSION CONDITIONS

a) *Semi-infinite linear diffusion*

The voltammetric responses would correspond to semi-infinite linear diffusion of M^{n+} ions in solutions and M atoms in the solid phase when the thickness of the liquid film or the radius of the liquid drop is sufficiently large (greater than 1 mm) and sufficiently fast sweep rates (greater than 100 mV/sec) are employed. Here are no practical difficulties in adhering to these experimental conditions especially when one considers the advantages as discussed below.

Under perfectly semi-infinite linear diffusion conditions, the voltammetric responses of the deposition-dissolution processes are the same as those of Ox/R reactions discussed earlier (Chapter 3). The characteristic cathodic peak potential, peak current, peak current ratios and peak separation values for reversible deposition/dissolution processes are again given by the expressions presented in Table 3.2. Of course, in these expressions C_{Ox} now corresponds to the metal ions in solution whereas C_R corresponds to the metal in the liquid medium It is easy to note that in the model level both the processes involve fast charge transfer and diffusion. The only difference is the direction of movement of reduced species which has no effect on the voltammetric response at all.

One caution must be exercised however in using equations of Table 3.2 for metal deposition/dissolution processes. The peak current ratio $i_{p,a}/i_{p,c}$ would be unity only if the diffusion coefficients of M^{n+} and M in their respective medium are equal. This would

not generally be true and hence the peak current ratio would vary. If one is sure that spherical diffusion and limited diffusion layer effects are absent (as seen later 6.3.1b), the peak current ratio would correspond to $(D_M/D_{M^{n+}})^{1/2}$ and hence it may be used to evaluate D_M in the metal.

Chemical equilibrium associated with reversible charge transfer (Section 6.2.2) may also be evaluated under these conditions by the methods discussed earlier (Section 3.4.6). For example, equation 3.61 can be directly used to evaluate the stability constants of metal complexes. When the ligand is present in large excess, this equation may be expressed in a more familiar form by substituting E^f values by $E_{1/2}$ values and thereby taking care of the inequality in the diffusion coefficients as follows :

$$E_{1/2,\ MX_p^{n+}} - E_{1/2,\ M^{n+}} = -\frac{0.059}{n} \log K - \frac{0.059}{n} \cdot \log X^p \quad 6.17$$

(Reaction 6.1 preceded by reaction 6.7).

In the study of metal-complex dissociation equilibrium by the above method, one must ensure that X is present in large excess and no uncomplexed metal ion exist. Recently some interesting CV simulation works were reported which could be used to evaluate the stability constants even when lower concentrations of ligands were present [17, 18]. The voltammetric peaks of free metal ion and complexed metal ions are very closely spaced so that no analytical expressions could be derived.

Under semi-infinite linear diffusion conditions, the methods developed for the study of irreversible charge transfer (Chapter 4) may also be directly used for deposition/dissolution processes. The boundary conditions (equations 6.3 and 6.4) are the same as the ones used for irreversible and quasi-reversible solution phase reactions respectively. Tables 4.2 and 4.3 may straightaway be employed for studying irreversible and quasi-reversible deposition/dissolution reactions. Interestingly the method developed for the study of quasi-reversible charge transfer [19] was first employed for the study of deposition/dissolution reaction (Cd deposition on Hg) rather than solution phase reaction [19, 20].

It is interesting to note that all the simulation studies of kinetics of chemical reactions in solution are also reported under semi-infinite linear diffusion conditions (Chapter 5). Hence the methods deve-

loped for reaction kinetics must also be applicable for deposition/dissolution reactions. The methods developed for *CE* reaction schemes (Section 5.3.1) must for example be applicable for the study of the kinetics of preceding reactions of the type 6.7. The *EC* reaction schemes (Section 5.3.2) must similarly be applicable for the chemical interactions in the metallic phase [16].

b) *Spherical diffusion conditions (HMDE)*

When metal deposition/dissolution studies are carried out with HMDE of smaller radii at lower sweep rate, one often notices that the anodic peak current is much larger than cathodic peak current or the $i_{p,a}/i_{p,c}$ is always greater than one. This can happen because of three reasons:

i) The diffusion coefficient D_M may be greater than $D_{M^{n+}}$

ii) When r_o the radius of HMDE is smaller, the assumption of planarity of the electrode surface becomes invalid.

iii) At longer times and smaller r_o values the assumption that the diffusion layer thickness L given by equation 6.16 is smaller than r_o also fails. The boundary condition of concentration of $M = 0$ as $y \rightarrow \alpha$ no longer holds. The effective concentration of M in the volume of the metal also increases to values that are larger than the bulk concentration of M^{n+} in solution and hence larger than the $i_{p,a}$.

Quantitatively the influence of r_o and sweep rate v on the voltammetric behaviour may be expressed by a dimensionless parameter p similar to 3.56.

$$p = r_o\,(nfv/D)^{1/2} \qquad 6.18$$

In this expression nfv or $nFv/\mathbf{R}T$ has a dimension of sec^{-1}. Therefore $1/nfv$ is the time response in *LSV* experiment. Hence

$$(nfv/D)^{1/2} = (1/Dt)^{1/2} = \sqrt{2/L} \qquad 6.19$$

using equation 6.16. Substituting this value in 6.18, we get

$$P = 2.r_o/L \qquad 6.20$$

This suggests that parameter p is essentially the ratio of radius of HMDE to diffusion layer thickness. If the ratio is very large, semi-infinite linear diffusion condition operates. If it is close to

unity the spherical correction must be considered. If p is much less than unity the limited volume effect also would predominate.

The first spherical diffusion correction to anodic dissolution process was suggested by Reinmuth [21]. The correction values tabulated earlier for solution phase processes [22] for various values of a dimensionless parameter ϕ (which is equal to $1/p$ of equation 6.18) could be employed for dissolution processes as well (Section 3). However, in contrast to solution phase processes, the metals are diffusing from a smaller volume of the sphere towards a larger volume and hence the spherical correction is negative [21]. Such a spherical correction was also established experimentally [23]. The complete LSV and CV response under spherical diffusion conditions were also numerically simulated [24].

All the above treatments considered spherical diffusion effects alone. However at slow sweep rates the influence of limited volume must be considered in addition to spherical diffusion. The peak currents $i_{p,a}$ and $i_{p,c}$ were related by the empirical expression 6.21 by Galus et al. [25, 26].

$$i_{p,a} = i_{p,c}\left[1 + 3.2\left\{\frac{D_M(E_{p,c} - E)}{r_o^2.v}\right\}^{1/2}\right] \qquad 6.21$$

This expression indicates that the $i_{p,a}$ would increase with increasing values of D_M and $E_{p,c} - E_\lambda$ (where E_λ is the cathodic switching potential) The $i_{p,a}$ would also increase with decreasing value of r_o and v. Experimental work as well as later simulation works [27] which took spherical diffusion as well as limited volume effects established that the above expression is essentially correct. Typical simulated CV curves for a reversible charge transfer for various p values defined by equation 6.18 are presented in Fig. 6.2.

Recently the general solution of CV curves for deposition/dissolution reactions on HMDE which takes into account the varying diffusion coefficients, spherical diffusion as well as limited electrode volume was reported [28]. Useful analytical expressions for $i_{p,c}$, $E_{p,c}$, $i_{p,a}/i_{p,c}$ as well as $E_{p,a}$ are given in this work (Table 6.1). These expressions can conveniently be used to calculate n, E^f ($E_{1/2}$), $D_M ne$ and D_M of reversible deposition-dissolution processes [28].

It must be noted that all the spherical diffusion effects considered so far were attempted only for reversible charge transfer. The

possible extensions to irreversible charge transfer and chemical reaction kinetics are even more involved. The experimentalist

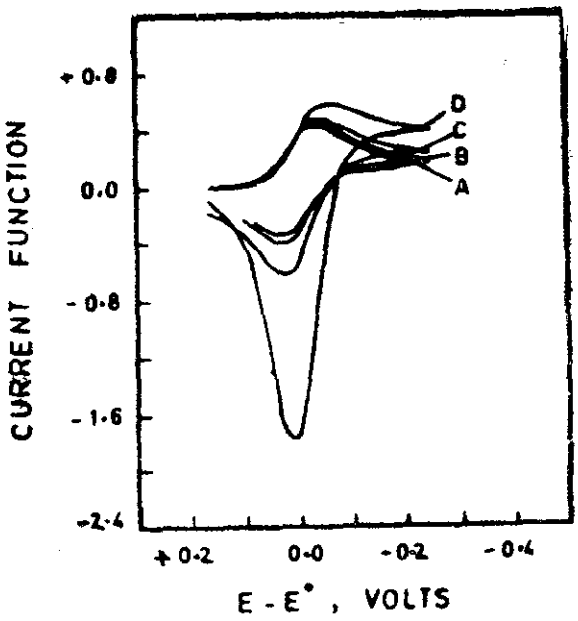

Fig. 6.2 Current functions versus potential curves for different values of $P = r_o\ (nfv/D)^{1/2}$ involving limited diffusion layer effect. p = (A) 137.74 (B) 43.67 (C) 13.79 (D) 4.40 Current function = $i_p/nFA\ CD^{1/2}\ v^{1/2}$

[From JE Spell and RH Philip Jr. Anal Chem 51 (1979) 2288]

interested in such work is of course recommended to work with semi-infinite linear diffusion conditions mentioned above (Section 6.3.1a)

6.3.2 VOLTAMMETRY ON THIN FILM PLANAR ELECTRODES

As is evident from the above discussions, the most important difference between the thick film and thin film electrode is the smaller volume of the latter. As a result of this thin film, the concentration of M in the liquid electrode becomes much greater than the concentration of $C_M n^+$ in solution. This has two effects for a reversible charge transfer. Because of a larger increase in product concentration, according to equation 6.2, the reduction

Table 6.1

Voltammetric behaviour of reversible deposition-dissolution processes under spherical diffusion conditions

Process: $M^{n+} + ne \rightleftharpoons M(\mathrm{Hg})$

$$i_{p,c} = 4\pi nFr_o^2(D_{M^{n+}}nfv)^{1/2} \times \{0.4463 + 0.741\, D_{M^{n+}}^{0.563} \cdot D_M^{-0.041}(r_o^2nfv)^{-0.522}\} \quad 6.1.a$$

$$E_{p,c} = E_{1/2} - \frac{RT}{nF}\left\{1.109 + 5.047 D_{M^{n+}}^{0.344} D_M^{0.168}(r_o^2nfv)^{-0.512}\right\} \quad 6.1.b$$

$$\frac{i_{p,a}}{i_{p,c}} = 1.000 + 4.130 \cdot D_{M^{n+}}^{0.172} D_M^{0.465}(r_o^2nfv)^{-0.637} \times \{(nf(E_{p,c} - E_\lambda)\}^{0.719} \quad 6.1.c$$

$$E_{p,a} = E_{1/2} + \frac{RT}{nf}\,[1.132 - 2.325 D_{M^{n+}}^{0.136} \cdot D_M^{0.442} \times (r_o^2nfv)^{-0.578}\{nf(E_{1/2} - E_\lambda)^{0.302}\}] \quad 6.1.d$$

potential (and hence E_p) shifts to more negative potentials. In addition, the anodic limiting current becomes much larger.

Theoretical simulation for LSV for the deposition on thin film electrode was carried out by de Vries and Van Dalen [29]. This was recently extended to cyclic voltammetry [30]. The influence of limited diffusion layer is treated by them by another dimensionless parameter H which is equal to p^2 where p is given by equation 6.18.

The peak current, peak potential and peak width values of deposition/dissolution process on a thin film electrode are presented in Table 6.2 [29, 30]. The cathodic peak current expression (6.2a) is very similar to the peak current expression for semi-infinite linear diffusion. The numerical constant value however is slightly less. The peak potential shifts cathodically if p is less than unity according to equation 6.2.b. The peak shape $(E_p - E_{p/2})$ however is independent of the thickness of the film (equation 6.2c).

Table 6.2

Voltammetric behaviour of reversible deposition/dissolution processes on thin film electrodes

Process:	$M^{n+} + ne \rightleftharpoons M_{film}$

Linear sweep voltammetry

$$i_{p,c} = 2.4953 \times 10^5 n^{3/2} \cdot A D_{M^{n+}}^{1/2} C_{M^{n+}} v^{1/2} \qquad 6.2.a$$

$$E_{p,c} = E_{1/2} - \frac{0.0385}{n} + 20.0295 \log \frac{l^2 n f v}{D_M} \qquad 6.2.b$$

$$E_{p,c} - E_{p/2,\,c} = \frac{65.54}{n} \text{ mV.} \qquad 6.2.c$$

Cyclic Voltammetry

$$\frac{i_{p,a}}{i_{p,c}} = \{0.9277 + 0.05042\, n(E_{p,c} - E_\lambda)\}^{1/2} \qquad 6.2.d$$

$$\Delta E_p = \frac{39.07}{n} + \frac{9.30}{n} \exp\{-0.009086\, n(E_{p,c} - E_\lambda)\} \text{ mV.} \qquad 6.2.e$$

$$\Delta W_{1/2} = \frac{75.53}{n} - 12.674 \exp\{-0.005226\, n(E_{p,c} - E_\lambda)\} \text{mV.} \qquad 6.2.f$$

In cyclic voltammetric experiments, the peak current ratio increases as the reverse potential becomes more negative (equation 6.2 d). The peak separation (equation 6.2 e) as well as the anodic peak width at half the anodic peak current 1/2 Δ W (Section 6.2.1) are also found to be dependent on E_λ. For these expressions to be valid, the reversing potential E_λ must be at least $(40/n)mV$ cathodic of $E_{p,c}$.

A typical CV curve for metal deposition/dissolution process on a thin film electrode is presented in Fig. 6.3. The excellent fit between the simulated and experimental curves may be noticed in this work [30]. The CV curve under semi-infinite linear diffusion conditions is also presented for comparison.

Again, no simulation studies of kinetic processes on thick film electrodes are available. For such works, one must reach semi-

infinite linear diffusion conditions at higher sweep rate or employ thick films (Section 6.3.1a).

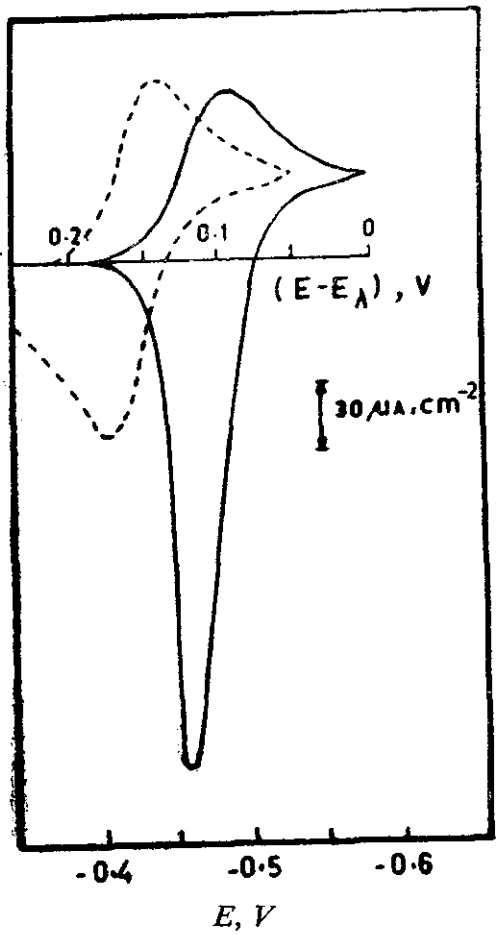

Fig. 6.3 Comparison of experimental (——) and theoretical (.....) CV curves obtained in a 0.3 M HCl containing 1×10^{-4} *M* of Pb^{2+} ions. Glassy carbon based mercury film electrode with $l = 0.7$ μm and surface area 0.05 cm^2. Dashed curve obtained at HMDE, Voltage scan 30 mV/sec.

[From M Donten, Z Stojek and Z Kublik, J Electroanal Chem 163 (1984) 11]

6.3.3 VOLTAMMETRY ON SOLID ELECTRODES

Bergin and Delahay [10] derived the LSV expressions for reversible metal ion deposition on a solid electrode of the same material where the product activity is assumed to be unity (6.5). The relevant peak current, and peak potential expressions are collected in Table 6.3. The peak current expression is again similar to the one for the deposition in the liquid electrode with the difference in the numerical constant (equation 6.3 a). The peak potential is dependent on the initial concentration of metal ion (equation 6.3 b). This is indeed a

Table 6.3

Voltammetric behaviour of reversible deposition of metal ion M^{n+} on its own solid substrate metal M

Process : $M_s + M^{n+} + ne \rightleftharpoons M_s - M$

$$i_{p,c} = 3.67\times10^5\times n^{3/2}\ \text{AC}\ v^{1/2}\ D^{1/2}_{M^{n+}} \qquad 6.3a$$

$$E_{p,c} = E^0 + \frac{0.0592}{n}\ [\log C_{M^{n+}} - \frac{0.0218}{n} \qquad 6.3b$$

$$E_{p,c} - E_{p/2,\,c} = \frac{21.8}{n}\ \text{mV} \qquad 6.3c$$

$$i_{p,a} \rightarrow \propto$$

very important characteristic for distinguishing deposition on solid electrode from other types of processes. The $E_p - E_{p/2}$ value is very narrow [31] when compared to other processes (equation 6.3 c). The cyclic voltammogram [32] also has a specifically different shape (Fig. 6.11). It must be noted that the dissolution process will not confine to deposited material but also the base electrode (Fig. 6.4).

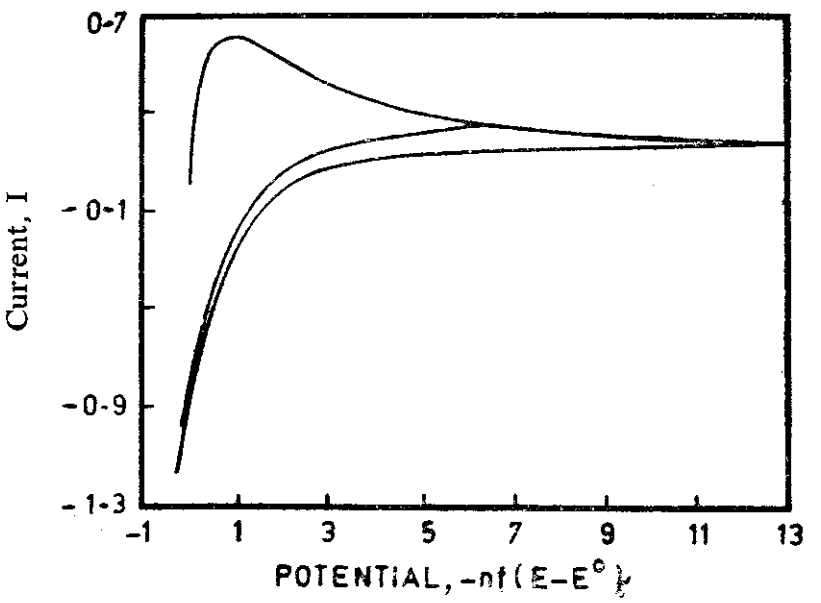

Fig. 6.4 Current function versus potential curves for metal ion deposition on the same metal electrode substrate.

[From N White and F Lawson, J Electroanal Chem 25 (1970) 409]

Although the theory developed above was for M^{n+}/M couple on the same electrode, thc initial experimental verifications were attempted for the deposition of one metal on another metallic substrate [10, 31, 33]. The unit activity conditions certainly will not apply for these systems, and hence the experimental results varied substantially from theory. The first attempts to explain these differences mainly depended on assuming the surface activity values less than one [10, 31, 33–35]. Attempts were made to experimentally evaluate such surface activities from measured voltammetric deviation [12, 36, 37]. However, it is now well-known that a number of phenomena could be involved when a metal is deposited on to another solid electrode such as electrochemisorption (Chapter 7), nucleation, growth, overlap (Chapters 7 and 8) and a number of phase transitions. And hence it is certainly not worthwhile to lump all these phenomena into one little 'activity coefficient' and continue 'explanation' type of theories. Solid state phase growth models and methods would be developed in the next chapter.

Interestingly enough, the LSV and CV theory of metal deposition/dissolution studies on the substrate electrode of the same type was recently verified for Ag^+ deposition on Ag [38, 39]. Theory as well as well-experimented verification of multisweep cyclic voltammetry are also reported [38, 39]. With gratification, it is noted that charge transfer and diffusion phenomena alone are able to explain the solid state phase growth at least in a handful of cases.

Simulated LSV and CV curves for deposition/dissolution processes on solid electrodes under irreversible charge tranfer conditions are also available [32]. The peak current decreases and the peak potential shifts cathodically with decreasing k^o values as is expected No analytical expressions for i_p, E_p and peak width are however available.

6.3.4 STRIPPING VOLTAMMETRY

Any stripping voltammetric procedure is made up of at least two steps, *a pre-concentration step* and a *stripping step*. In the anodic stripping voltammetry for example, the pre-concentration step is a cathodic deposition step. The total amount of metal deposited in this step may be easily estimated by measuring the total electric charge consumed (coulometry) or by integrating the current-time

response during the entire period of pre-concentration. This step essentially increases the bulk concentration of metal in the electrode. By proper choice of the experimental variables (deposition potential, time, thickness or radius of the liquid electrode, eleetrolyte flow rate, the rpm of the solid or film electrode) the concentration may be enhanced by 1000 times. It is this enhanced concentration that offers the highest sensitivity during analysis (Section 6.5). The second essential step, the stripping of the preconcentrated metal may be carried out in a number of possible ways. In this work, the concern is only with the stripping voltammetric response when a linear potential sweep is employed. In between the two steps mentioned above, a rest-time is usually allowed to ensure steady state condition in electrolyte as well as in the electrode (uniform concentration distribution of M in the liquid electrode). In this section the methods of evaluating voltammetric response shall be considered in some detail.

a) *Stripping from HMDE*

The stripping voltammetric response again depends very much on the nature of electrode material employed. The anodic stripping voltammogram obtained from HMDE is quite similar to the cathodic response [21–24]. The spherical diffusion effects would predominate only at very slow sweep rates, and even in such cases the spherical correction methods discussed above (Section 6.3.1b) may be directly employed. However, since the current response increases with $v^{1/2}$ and the spherical corrections are also absent at higher sweep rates [21–24], it is preferable to carry out ASV analysis on HMDE at fairly high sweep rates. At very high sweep rates the contribution from double layer charging would of course interfere. This can be eliminated by measuring the derivative current di/dt as a function of potential [40].

Some empirical as well as semi-quantitative approaches were made to quantitatively predict the ASV response with parameters of pre-concentration steps such as pre-electrolysis time and deposition potential [41, 42]. However, these attempts led to very limited success because the number of experimental variables involved are really too many to be amenable to the quantitative approach. It is much easier to employ the peak current expressions 6.22 and 6.23 for reversible and irreversible charge transfer respectively for the eva-

luation of C_M, D_M, n and αn_a, knowing other parameters.

$$i_{p,a\cdot\text{rev.}} = -2.69 \times 10^5 \times n^{3/2} AC_m v^{1/2} D_M^{1/2} \qquad 6.22$$

$$i_{p,a,\text{irr.}} = -2.98 \times 10^5 \times n(\alpha na)^{1/2} AC_M v^{1/2} D_m^{1/2} \qquad 6.23$$

b) *Mercury film etectrode (MFE)*

The anodic dissolution of metals from thin film electrode was considered in detail by de Vries and Van Dalen [11, 43, 44]. The main difficulty in finding analytical expressions for i_p, E_p etc. is the modelling of the concentration gradient in the liquid metallic film for C_M. This problem is greatly simplified if one assumes that the film thickness is very much smaller when compared with the diffusion layer thickness [29, 45]. This essentially means that the dimensionless parameter p' (given in equation 6.24) is very much smaller than 1.

$$p' = l(nfv/D)^{1/2} \qquad 6.24$$

Note the similarity between this parameter p' and the dimensionless parameter p given by equation 6.18. Both the parameters, of course, relate to the ratio of film thickness to the time dependent diffusion layer thickness (note the dimensions following equation 6.18).

When $p' \ll 1$ is satisfied, one may obtain the simplified expressions for the ASV of thin film metal deposits [29]. The relevant voltammetric characteristics at 298K are collected in Table 6.4. The peak is now directly proportional to v (equation 6.4a). This is an important diagnostic criteria which distinguishes it from diffusion limited currents (i_p is proportional to $v^{1/2}$). Equation 6.4a also suggests that i_p is independent of D_M. This is because $p' \ll 1$ essentially implies that during the anodic sweep all the metal atoms (M) present in the thin film are completely dissolved. The total charge required for dissolving all the metal ions are given by equation 6.4b. q_m may be easily obtained by integrating ASV curve. Substituting equation 6.4b in 6.4a another expression may be obtained for $i_{p,a}$ (equation 6.4c). The peak potential is found to depend on the film thickness and sweep rate (equation 6.4d). The peak width at half peak height however is found to be independent of these parameters (equation 6.4e).

The voltammetric behaviour of anodic dissolution of metals in thin films when the charge transfer is irreversible has also been evaluated [46]. The peak current (equation 6.4f) and the peak potential (equation 6.4g) now depend on the transfer coefficients as well. A general mathematical treatment for handling all the range of film thickness values (finite film thickness model to semi-infinite linear diffusion model) is also available [47].

The ASV of a number of metals from mercury film electrodes were carried out with the primary objective of verifying the voltammetric expressions given in Table 6.4 [48–50]. Under reversible charge transfer conditions the agreement between experiment and

Table 6.4

Voltammetric behaviour of dissolution of metals from thin films.

Process : $M^{n+} + ne \rightleftharpoons M_{film}$

Reversible charge transfer :

$$i_{p,a} = 1.1157 \times 10^6 \, n^2 \, A \, C_M \, l \, v \qquad 6.4a$$

$$q_m = nF \, Al \, C_M \qquad 6.4b$$

$$i_{p,a} = 11.6 \, n. \, q_m. \, v \qquad 6.4c$$

$$E_{p,a} = E_{1/2} - \frac{1.43}{n} + \frac{29.58}{n} \log \frac{l^2 nfv}{D_M}. \text{ mV.} \qquad 6.4d$$

$$\Delta W_{1/2} = \frac{75.53}{n} \text{ mV} \qquad 6.4e$$

Irreversible charge transfer :

$$i_{p,a} = 1.422 \times 10^6 \, n \, (\alpha n_a) \, A \, C_M \, lv \qquad 6.4f$$

$$E_{p,a} = E_{1/2} + \frac{0.059}{\alpha n_a} \log \frac{lnfv}{k_h^o} \qquad 6.4g$$

theory was found to be excellent as long as the C_M in Hg does not exceed its solubility.

The sensitivity of MFE may be further improved by carrying out differential pulse voltammetry (*DP* ASV). The theory as well as experimental verification has been worked out by Osteryoung and co-workers [51-53].

c) *Solid electrodes*

The ASV benaviour of thin solid metal films again may be given by the expressions in Table 6.4 [54, 55]. However, for these systems the thickness d now refers to the thickness of the dissolving metallic layer. These expressions would hold only if the activity of M on the substrate is always unity and if the solid metal film is uniform throughout. As noted earlier, attempts were made to incorporate activity effects [36, 37]. Quantitative analysis involving the preconcentration steps were also attempted [54, 55]. However the resulting expressions are much more involved.

The voltammetric behaviour of thin film of electroactive particles formed as an active paste on a carbon substrate for example is similar to the expressions presented in Table 6.4 [56, 57]. The parameter l now refers to the average thickness of the electroactive particles. The treatment [56, 57] again assumes that the particle film is uniform throughout and only one layer of active particles dissolves in a stripping step.

All the discussions about voltammetric methods in this section (6.3.4) are based on the assumption that the concentration (or activity) of the metal throughout the liquid electrode, liquid film or solid film is uniform. The experimental results would vary whenever this condition is not obeyed. Conversely the variation in metallic activity, the formation of non-uniform phase due to deposition of metal exceeding its solubility limit may be directly established whenever deviation from the above behaviour is noticed (Section 6.4.3).

6.4 THE PROCESS

6.4.1 THE CHARGE TRANSFER

As noted earlier (Section 6.3.1), the LSV and CV methods for the analysis of charge transfer thermodynamics and kinetics of deposi-

tion/dissolution on HMDE are very much similar to the ones used in solution phase processes (Tables 3.2 and 4.2). The first application of Nicholson's method [19] of evaluating k_h^o was made for *Cd* deposition/dissolution processes [19, 20]. However these methods are now widely used for the study of solution phase reactions alone (Chapters 4 and 11). The charge transfer kinetics of fairly fast deposition/dissolution reactions (which are reversible under polarographic time scales) certainly deserve much more detailed consideration than given at present. In fact, LSV and CV methods may easily be applied for studying these reactions in detail and establishing the potential dependence of transfer coefficient (Section 4.4) and obtaining linear free energy relation.

Deposition/dissolution processes on Hg have received some attention in the recent past. The solvent effects on charge transfer kinetics is being considered in detail by Galvs and his co-workers [58–60]. The electrochemical behaviour of Cu^{2+} and Cu^{+} species in low temperature melt has also been evaluated [61]. These studies only point to the extensive scope for studies in this direction. However, it must be made clear at this stage that the models and methods developed here are applicable for the studies on Hg electrode or similar liquid electrode alone. On solid electrodes one must also consider other phenomena such as nucleation growth [62]. Such models are considered in a later chapter (Chapter 8).

Anodic deposition of halides on Hg may also be described by the methods developed above if the Hg salts or compounds formed are soluble in bulk Hg. In this direction also very little progress has been made [63, 64]. If the oxidation product is insoluble in bulk mercury then the film would probably correspond to monolayers. The methods for the study of such systems would be considered later (Chapter 7), However, for bulk deposition the anodic peak current would depend on $C_{\boldsymbol{x}}$- and $v^{1/2}$ according to equations 6.22 or 6.23. For monolayer film formation studies, the mass transfer effects would be absent.

6.4.2 CHEMICAL REACTIONS IN SOLUTION

The study of metal complex formation equilibrium (6.7) in solution still remains as one of the major applications of polarographic technique [13–15]. If the reduction process is reversible under polaro-

graphic conditions, the $E_{1/2}$ changes with the concentration may be easily determined by polarographic techniques. A great deal of continuous research is going on in this area and it would remain to grow.

However, there are at least a few occasions when the LSV and CV techniques would be of advantage. Voltammetric responses in in presence of low levels of ligand concentrations may be evaluated by CV techniques much more precisely [17, 18]. Numerical simulations are of course required for such works. When the metal ions are also present in very low levels, the stability constants of metal complexes may be evaluated from the anodic stripping voltammograms [65–66]. The methods employed are of course quite similar to the voltammetry of deposition step employed usually [13–15].

With increasing use of non-aqueous solvents in electrochemistry, the influence of solvent molecules in the metal deposition processes have received some attention. The solvents that are more basic than water stabilize the metal ions in the solvent [58–60, 67, 68]. The free energy of transfer of the solvent can be determined again by the shift in $E_{1/2}$ or E^f with solvent concentration in a mixed solvent medium [58–60]. Linear relation also seems to exist between the solvation free energy and the heterogeneous charge tranfer rate constant k_h^o [58–60].

In a large number of voltammetric studies of metal complexes, the complex formation as well as dissociation steps are assumed to be in equilibrium.

However, at least in low levels of ligand concentrations and high sweep rates, the chemical dissociation of the metallic complex may be a slow step. The dissociation kinetics of even very fast chemical reactions of this type may be studied by LSV and CV techniques (*CE* mechanism—Chapter 5). The CV curves in Fig. 6.5 at higher *DMSO* concentrations for example show that the cathodic sweep contains a limiting wave. The chemical dissociation of the Ni^{2+}-solvent complex seems to be a slow step in this case [59]. There is wide scope for further studies in this direction.

6.4.3 DIFFUSION OF METALS IN MERCURY

The diffusion coefficients of metals in mercury may be evaluated by measuring the ASV of the metal on HMDE and using relations

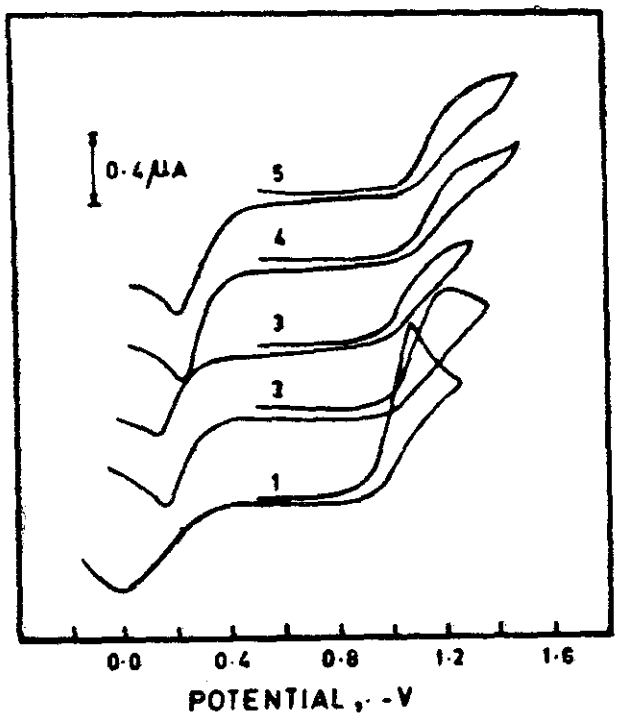

Fig. 6.5 Cyclic voltammetric curves of 4×10^{-4} M Ni^{2+} in 0.4M $NaClO_4$. Concentration of DMSO curve (1) 0; (2) 10; (3) 50; (4) 90; (5) 100 % Sweep rate 25 mV/sec

[From L Janiszewska and Z Galus, Electrochim Acta 29 (1984) 1419]

6.22 or 6.23. One must however first know whether the dissolution process is reversible or irreversible. This difficulty is avoided in a closely related technique of chronoamperometry. In this technique the deposition potential is taken from the deposition potential to sufficiently anodic potential to ensure complete control by mass transfer. The current-time response under this condition is given by equation 6.25

$$i = nFAC_M D^{1/2}/\pi^{1/2} t^{1/2} \qquad 6.25$$

This equation suggests that i versus $t^{-1/2}$ [69] or $it^{1/2}$ versus $t^{1/2}$ plot would be linear 6.25 [70]. It may be noted that this is independent of the rate of charge transfer.

The diffusion coefficient of a number of metals that can be deposited on Hg electrodes are presented in Table 6.5 [71, 72]. The validity of the diffusion coefficient data was confirmed recently [73]. The diffusion coefficients of metal ions in solution may be determined by the above method under the mass transfer controlled deposition

Table 6.5

Diffusion coefficients of metals in mercury at 20°C

Metal	Background electrolyte	Diffusion coefficient $D \times 10^5$(cm^2/sec)
Cu	1M HNO_3	1.19 ± 0.2
Bi	1M $HClO_4$	1.44 ± 0.06
Sb	1M H_2SO_4	1.52 ± 0.02
		2.42 ± 0.03 (at 90°C)
Pb	2M $HClO_4$	1.25 ± 0.04
Sn	5M HCl	1.48 ± 0.04
Ni	6M $CaCl_2$	0.64 ± 0.02
Tl	1M HNO_3	0.91 ± 0.07
In	1M HCl	1.36 ± 0.07
Cd	1M KCl	1.42 ± 0.05
Ga	Sat. NH_4COOCH_3	1.72 ± 0.07
Zn	1M KCl	1.89 ± 0.04
Mn	6M $CaCl_2$	0.94 ± 0.03
Na	Sat. NaOH	0.97 ± 0.1
K	Sat. KOH	0.85 ± 0.06
Rb	Sat. RbOH	0.75 ± 0.08
Cs	Sat. CsOH	0.54 ± 0.08
Ba	Sat. $BaCl_2$ & $Ba(OH)_2$	0.49 ± 0.09

conditions. However, unlike D_M, the $D_{M^{n+}}$ values depend on a number of experimental variables such as solvent composition, supporting electrolyte concentration and nature and size of the ligand employed. In this sense the D_M values are much more independent of experimental conditions. Hence D_M values may for

example be used to evaluate the purity of electrodes and the influence of non-spherical diffusion [28].

6.4.4 THE METAL-METAL INTERACTIONS

The solubility of a metal in Hg (or in any other liquid metal for that matter) would certainly depend on the nature of the metal [74]. Metals such as In, Tl, Cd and Pb are highly soluble and hence their voltammetric behaviour would correspond to theoretical predictions even if the concentration of these metals in Hg are very high. However, other metals such as Cu, Ni and Co are much less soluble. They might form a distinct non-homogeneous phase in Hg whenever their solubility is exceeded. The voltammograms are then less reproducible and the anodic waves become much broader. The solubility limitations are even more severe when thin film electrodes are used [48–50, 75]. Solubility limitation may have to be considered even when the deposition of highly soluble In metal in a thin film of Hg is taken up [75].

In addition to the solubility effects, chemical interactions between Hg and the deposited metal must also be considered. The alkali metals, for example, are deposited on Hg at much more positive potentials when compared with standard reduction potentials. Such studies are in fact very useful in understanding the metal-mercury interactions properly.

When more than one metal (M_1 and M_2) are deposited on Hg, the M_1-M_2 chemical interactions must be considered. Intermetallic compounds are often formed whenever a noble metal such as Au or Cu is co-deposited with an active metal such as Zn or Cd. The deposited active metal, for example, is stabilized by such intermetallic compound formation and hence is oxidized at much more positive potential when compared with the dissolution in the absence of noble metal. The influence of Pt based mercury drop electrodes on the ASV of active metals was established in very early times [16]. The intermetallic compound formation equilibrium has received some detailed consideration recently [77, 78]. Intermetallic compound formation may also be put to analytical advantage for suppression of one of the two closely spaced peaks [79].

The intermetallic compound formation in mercury may be viewed as a second order chemical reaction following charge transfer. The

rate of such reactions may be analyzed by the methods developed for the *EC* reaction schemes in solution (Chapter 5). There is ample scope for further research in this direction.

6.5 ANALYTICAL APPLICATIONS AND SCOPE

Among the analytical applications being considered in the entire work, stripping analysis in general and anodic stripping voltammetry in particular are certainly the most successful and widely used ones. This is due to the possibility of carrying out two analytical functions in the same experimental set-up. The metal concentration can be enhanced substantially (say 1000–fold or more) in a pre-electrolysis step. The analysis is then carried out in the stripping step. The overall effect is that detection and estimation limit goes to 10^{-9} to 10^{-10} moles/litre. Thus this method competes very well with other comparative methods.

Excellent review works of varying size, content and emphasis on stripping voltammetry have appeared over the past several years [16, 57, 72, 80–87]. The experimental methodology as well as the collected tables of analysis of various samples may be found in these works. Detailed considerations of preparation of HMDE [88], solid carbon [89] as well as mercury thin film electrodes are now available [90–93]. The Hg film electrodes are of course more sensitive when compared with HMDE both in terms of resolution and sensitivity [91] (Fig. 6.6). On Hg electrode one can now detect a number of metal ions such as Bi^{3+}, Cd^{2+}, Cu^{2+}, Ga^{3+}, Ge^{4+}, In^{3+}, Ni^{2+}, Pb^{2+}, Sb^{2+}, Sn^{2+}, Tl^{+} and Zn^{2+}. Alkali metals may be estimated with slightly lesser level of accuracy. The solid electrodes may be used to determine the noble metals including platinum and mercury. It is neither possible nor desirable to survey the entire analytical aspects here. However, a few representative advances in recent times would be cited to point out present state of affairs in this area.

In anodic stripping voltammetry attempts are being made to construct automatic devices to carry out mixed element analysis [94]. Attempts for direct estimation of sea water samples [95] and even estimation of samples without the requirement of deaeration [96] are being made. ASV technique has also been used to evaluate metal ion concentrations in flowing solutions [97]. This type of approach may find use in flow-through detectors of liquid chromatography.

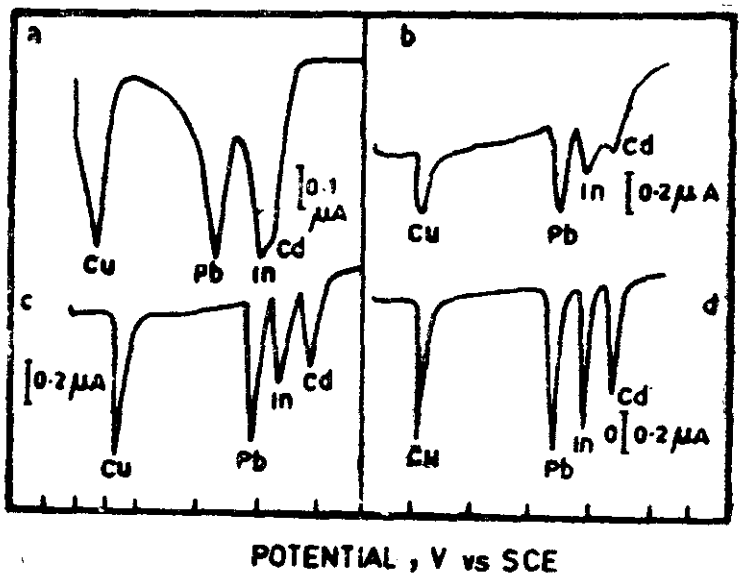

Fig. 6.6 Effect of substrate (a) Hanging mercury drop, 30 min. deposition, (b) Pyrolytic graphie, 5 min. deposition, (c) Unpolished glassy carbon, 5 min. deposition, (d) Polished glassy carbon, 5 min, deposition.

All contained 2×10^{-7}M Cd^{2+}, In^{3+}, Pb^{2+} and Cu^{2+} in 0.1 M KNO_3. Scan rate 5 mV/sec. Solution for *b*—*d* also contained 2×10^{-5}M Hg and were rotated at 2000 rpm.

[From TM Florence, J Electroanal Chem 27 (1970) 273],

Cathodic stripping voltammetry in which anion and organic compounds are pre-concentrated by anodic oxidation on Hg and cathodically stripped for analysis was introduced very much later when compared with ASV [98, 99]. However, the progress in this area is indeed very fast. At present, it is possible to estimate a number of anions such as halides, sulphides, selenides, chromates, oxalates, succinates and diethyl thiophosphates by this method. CSV is also used for the analysis of biological samples [100, 101]. Solid samples of oxides, and sulphides of a number of metals may be analyzed by forming a thin film of these materials on carbon electrodes [72]. Although the mechanistic aspects of these reactions are not well understood at present, the analytical applications have developed substantially [72].

If the electroactive compound in solution can be easily adsorbed on an electrode surface without any charge transfer, the pre-concentration can be carried out by holding the electrode for a stipulated time. This type of stripping voltammetry is now termed as adsorptive stripping voltammetry [87, 102–104]. The concentration

of adsorbed species are also linearly related to the peak current. However, the complete voltammetric curve are however described by different expressions corresponding to monolayer redox processes (Chapter 9). So far the direct analytical applications of deposition/dissolution processes have been considered. Attempts to develop voltammetric techniques for monitoring metal plating operations are being made in recent times [105, 106]. These approaches might play a very important role in monitoring and controlling the bath composition in future plating baths.

In this chapter then, the surface processes have been considered that can be described by the three phenomenological model components, charge transfer, chemical reaction and mass transport. In the next chapter the surface processes shall be considered in a more microscopic—in fact monolayer-level. Many new model parameters would of course have to be introduced. But we are in fact studying the processes at the atomic level of interactions—a very interesting possibility indeed.

REFERENCES

1 LA Mattison and N Nichols, Trans Electrochem Soc 73 (1938) 193.
2 KW Gardiner and LB Rogers, Anal Chem 25 (1953) 1393.
3 TL Marple and LB Rogers, Anal Chim Acta 11 (1954) 574.
4 W Kemula and Z Kublik, Roczmiki chim 32 (1958) 941.
5 W Kemula, Z Galus and Z Kublik, Roczmiki chim 33 (1959) 1431.
6 SS Lord, RC O'Neil and LB Rogers, Anal Chem 24 (1952) 209.
7 ES Jacobs, Anal Chem 35 (1963) 2112.
8 JEB Randles, Trans Farad Soc 44 (1948) 327.
9 A Seveik, Collect Czech Chem Commum 13 (1948) 349.
10 T Berzmiand P Delahay, J Am Chem Soc 75 (1953) 555.
11 WT de Vries and E Van Dalen, J Electroanal Chem 8 (1964) 366.
12 Kh Z Brainina, NK Kiva and VB Belyavskaya, Elactrokhimyia 1 (1965) 311.
13 AA Vlcek, Prog in Inorg Chem Vol. 5 (FA Cotton, Ed) Interscience, N York (1963) 211.
14 J Koryta in Adv in Electrochem and Electrochem Eng 5 (1967) 283.
15 DR Crow, Polarography of metal complexes, Academic Press, N York (1969).

16 W Kemula in Advances in Polarography, Vol. 1 (IS Longmuir, Ed). Pergamon, London (1960) 105.
17 JE Spell and RH Philip, Jr. J Electroanal Chem 112 (1980) 281.
18 HM Killa, EE Mercer and RH Philp, J. Anal Chem 56 (1984) 2401.
19 RS Nicholson, Anal Chem 37 (1965) 1351.
20 SP Perone, Anal Chem 38 (1966) 1158.
21 WH Reinmuth, Anal Chem 33 (1961) 185.
22 WH Reinmuth, J Am Chem Soc 79 (1957) 6358.
23 I Shain and J Lewinson, Anal Chem 33 (1961) 187.
24 FH Beyerlein and RS Nicholson, Anal Chem 44 (1972) 1647.
25 C Guminski and Z Galus, Roczniki Chem 43 (1969) 2147.
26 Z Galus, Fundamentals of Electrochemical Analysis, Harwood Chichester, Susses, England (1976)
27 JE Spell and RH Philip Jr. Anal Chem 51 (1979) 2288.
28 K Tokuda, N Enomoto, H Matsuda and N Koizumi, J Electroanal Chem 159 (1983) 23.
29 WT de Vries and E Van Dalen, J Electroanal Chem 14 (1967) 315.
30 M Donten, Z Stojek and Z Kublik, J Electroanal Chem 163 (1984) 11.
31 G Mamantov, DL Manning and JM Dale, J Eleetroanal Chem 9 (1965) 253.
32 N White and F Lawson, J Electroanal Chem 25 (1970) 409.
33 N White and F Lawson, J Electroanal Chem 26 (1970) 113.
34 MM Nicholson, J Am Chem Soc 79 (1957) 7.
35 MM Nicholson, Anal Chem 32 (1960) 1058.
36 Kh Z Brainina, NF Zakharchuk, DP Synkova and IG Yudelevich, J Electroanal Chem 33 (1972) 165.
37 Kh Brainina, Talenta 18 (1971) 513.
38 PC Andricocos and PN Ross, Jr., J Electrochem Soc 130 (1983) 1353.
39 PC Andricocos and PN Ross, Jr. J Electrochem Soc 131 (1984) 1531.
40 CV Evans and SP Perone, Anal Chem 39 (1967) 309.
41 AG Stronberg, Zavadsk lab 29 (1963) 387.
42 G Huderova and K Stulik. Talenta 19 (1972) 1258
43 WT de Vries, J Electroanal Chem 9 (1965) 448.
44 WT de Vries and E Van Dalen, J Electroanal Chem 12 (1966) 9.
45 DK Roe and JE Toni, Anal Chem 37 (1965) 1503.
46 RV Bucur, I Covaci and C Miron, J Electroanal Chem 13 (1966) 263,
47 HE Keller and WH Reinmuth, Anal Chem 44 (1972) 434.
48 Z Stajek, B Stepnik and Z Kublik, J Electroanal Chem 74 (1976) 277.
49 Z Stojek and Z Kublik, J Electroanal Chem 77 (1977) 205.
50 P Ostrapczuk and Z Kublik, J Electroanal Chem 93 (1978) 195.

51 RA Osteryoung and JH Christie, Anal Chem 46 (1974) 351.
52 U Eisner, JA Turner and RA Osteryoung, Anal Chem 48 (1976) 1608.
53 M Penczek, Z Stojek and J Osteryoung, J Electroanal Chem 170 (1984) 99.
54 Kh Z Brainina, and GV Yarunina, Electrokhimya 2 (1966) 781.
55 Kh Z Brainina, Elektrokhimyia 2 (1966) 1006.
56 Kh Z Brainina and RP Lesunova, Zh Anal Khim 29 (1974) 1302.
57 Kh Z Brainina and Mr Vydrevich, J Electroanal Chem 121 (1981) 1.
58 J Broda and Z Galus, Electrochim Acta 23 (1983) 1523.
59 L Janiszewska and Z Galus, Electrochim Acta 29 (1984) 1419.
60 J Stroka, K Maksymluk and Z Galus, J Electroanal Chem 167 (1984) 211.
61 C Nanjundiah and RA Osteryoung, J Electrochem Soc 130 (1983) 1312.
62 VN Ngac, O Vittori and G Quarin, J Electroanal Chem 167 (1984) 227.
63 P Kiekens, MLC Mertens and E Temmerman, Analyst 108 (1983) 1082.
64 M Wojciechowski and J Osteryoung, Anal Chem 56 (1984) 1884.
65 HC Budnikov, VA Vlakhovich and IV Postnova, J Electroanal Chem 154 (1983) 171.
66 M Valenta, HW Nurnberg and T Kambona, J Electroanal Chem 180 (1984) 343.
67 J Dandoy and L Gierst, J Electroanal Chem 2 (1961) 116.
68 GJ Hills and LM Peter, J Electroanal Chem 50 (1974) 175.
69 H Kao aud CG Chang, Acta Sci Natural Univ Nankinensis 9 (1965) 326.
70 WG Stevens and I Shain, J Phys Chem 70 (1966) 2276.
71 A Baranski and Z Galus, J Electroanal Chem 60 (1975) 175.
72 Z Galus, CRC Crit Rev Anal Chem 4 (1975) 359.
73 XS Ma, H Kao and CG Chang, J Electroanal Chem 151 (1983) 179.
74 M Kozlovsky aud A Zebrova in Progress in Polarography Vol. 3 (P Zuman and L Meites, Ed.) Wiley-Interscience, N York (1972) 166.
75 K Wilkiel and Kublik, J Electroanal Chem 161 (1984) 269,
76 L Ramaley, RL Brubaker and CG Enke, Anal Chim 35 (1963) 1088.
77 JA Wise, DA Rostan and WR Heineman, Anal Chim Acta 154 (1983) 95.
78 EY Nieman, LG Petrova, VI Ignatov, GM Dolgoplova, Anal Chim Acta 113 (1980) 277.
79 J Nang, PAM Farias and DM Luo, Anal Chim 56 (1984) 2379.
80 E Barendrecht in Electroanalytical Chemistry, 2 (1967).
81 Kh Z Brainia, Stripping Voltammetry in Chemical Analysis, Wiley Interscience, New York (1974).
82 TR Copeland and RK Skogerboc, Anal Chem 46 (1974) 1257 A.

83 F Vydra, K Stulik and E Julakova, Electrochemical Stripping Analysis, Wiley Interscience, New York (1976).
84 WR Heineman, HB Mark Jr, JA Wise and DA Roston in Laboratory Techniques in Electroanal Chem (PT Kissinger and VR Heineman, Ed.) Marcel Dekker, N York (1984) 499.
85 TM Florence, J Electroanal Chem 168 (1984) 207.
86 TP Radhakrishnan in Workshop on Electrochemistry (R Sundaresan and MK Totlani, Ed,) SAEST Bombay Chapter, Bombay, India (1985) 77.
87 J Wang, Stripping Analysis: Principles, Instrumentation and Applications, Verlag Chemie, Dearfield Beach, Weinkein (1985).
88 Z Galus in Laboratory Techniques in Electrochemistry (PT Kissinger and WR Heineman, Ed.) Marcel Dekker, N York (1984) 267.
89 G Dryhurst and DL McAllister, ibid, 289.
90 N Winograd, ibid. 321.
91 TM Florence, J Electroanal Chem 27 (1970) 273.
92 GE Batley and TM Florence, J Electroanal Chem 55 (1974) 23.
93 RG Clem, G Litton and LD Ornelas, Anal Chem 45 (1973) 1306.
94 DR Turner, SG Robinson and M Whitfield, Anal Chem 55 (1984) 2387.
95 A Nelson and RFC Mantoura, Electroanal Chem 164 (1984) 253.
96 M Wojciechowski, W Go and J Osteryoung, Anal Chem 57 (1985) 155.
97 GW Schieffer and W J Blaedel, Anal Chem 49 (1977) 49; 50 (1978) 99.
98 HA Laitinen and NH Watkins, Anal Chem 47 (1975) 1352.
99 BL Dennis, J Moyers and GS Wilson, Anal Chem 48 (1976) 1611.
100 MO Rozali, J O Hill and RJ Magee, J Electroanal Chem 168 (1984) 219.
101 H Klukanova, M Studnickova and J Kovar, Bioelectrochem Bioenerg 12 (1984) 279.
102 J Wang and PAM Farias, J Electroanal Chem 182 (1985) 211.
103 J Wang and BA Faeiha, J Electroanal Chem 151 (1983) 273.
104 J Wang, DB Luo, PAM Farias and JS Mahmoud, Anal Chem 57 (1985) 158.
105 W Bauer, M Butz and CJ Raub, Metalloberflache 38 (1984) 515,.
106 ML Rothstein, Plating Surf Finish 71 (1981) 36.